Desalination and Water Treatment
www.deswater.com
doi: 10.5004/dwt.2022.29042

277 (2022) 305–315
November

Fabrication removal method of gallic acid and Pb^{2+} ions in real samples by a new adsorbent chitosan grafted with a mixture of itaconic acid-methacrylamide

Fariborz Azizinezhad

Department of Chemistry and Chemical Engineering, College of Science, Varamin-Pishva Branch, Islamic Azad University, Varamin, Iran, Tel. +98 9127216112; email: fazizinejad@yahoo.com/fazizinejad@iauvaramin.ac.ir

Received 13 June 2022; Accepted 18 October 2022

ABSTRACT

In this study, chitosan (CTS) with medium molecular weight, using a mixture of monomers, itaconic acid (IA) and methacrylamide (MAm) were grafted in the presence of radical initiator, 4,4′-azobis(4-cyanovaleric acid) (ACV) and ethylene glycol dimethacrylate (EGDMA) as cross-linkage. The best graft yield was obtained by gravimetric method (EGDMA = 2 mL, ACV = 0.01 g, IA = 0.01 g, MAm = 0.09 g, t = 45 min, CTS = 0.2 g. The characterization was performed by X-ray diffraction, Fourier-transform infrared spectroscopy, thermogravimetric analysis and scanning electron microscopy methods. The composite was used to adsorb Pb^{2+} and gallic acid compounds and important adsorption parameters including pH, adsorption time, adsorbate concentration and adsorbent amount were optimized. The best adsorption conditions for Pb^{2+} (time = 75 min, pH = 4.0, adsorbent = 0.05 g, adsorbate concentration = 150 mg/L and q_{max} = 276 mg/g) and for gallic acid (time = 60 min, pH = 3.0, adsorbent = 0.02 g, adsorbate concentration = 300 mg/L and q_{max} = 576 mg/g) were recorded. The adsorption data's were fitted by Langmuir isotherm and pseudo-second-order kinetic model, as well. Thermodynamic studies showed that the adsorption process is endothermic and spontaneous and due to the increase in entropy confirms the proper interaction of the adsorbent and adsorbate. Meantime, due to the high adsorption capacity of the adsorbent and good efficiency after several times of adsorption–desorption, it can be used as an industrial adsorbent.

Keywords: Chitosan; Itaconic acid; Methacrylamide; Adsorption

1. Introduction

Chitosan is obtained by N-deacetylation of chitin with strong alkali [1]. It is a natural adsorbent for metal ions such as zinc, nickel, copper, chromium and lead. This could be for the following reasons: Large group of hydroxyl in chitosan, existence of primary amino groups that are considered as adsorption sites, and the flexibility of a polymer chain structure that works as a convenient provider for the formation of complexes with metal ions [2]. All toxic metals can be absorbed by living organisms. Large amounts of these metals accumulate in the human body through the food chain. Due to the digestion of these metals in the body, they can cause some health problems and disorders in humans and animals [3]. Pb is a toxic metal that accumulates and enters the vital organs of humans and animals. It enters the body through air, water and food. According to the World Health Organization's (WHO) standards, its maximum limit in drinking water is 0.05 mg/L and in wastewater is 0.5 mg/L [4]. The presence of small amounts of toxic metal ions in liquid solutions is challenging. In addition, the method of separating metal ions from wastewater is a complex process

by pH, competing ions, and the presence of organic substances. Various methods such as filtration, ion exchange, precipitation and adsorption have been used to remove toxic species from liquid solutions [5–8]. Chemical modification of natural polymers is a good way to produce new, high-performance biomaterials. Various articles have been published on graft copolymerization of acrylonitrile, dimethylaminoethyl methacrylate, acrylamide, and vinylpyrrolidone onto chitosan using ceric ammonium nitrate (CAN) as an initiator [9–13]. On the other hand, γ-Ray and photoinduced graft-copolymerization of acrylamide, methyl methacrylate, 2-hydroxyethyl methacrylate, styrene and acrylonitrile on chitosan has also been reported [10–14]. Chitosan is grafted using potassium persulfate as a redox initiator of methyl methacrylate, methyl acrylate, butyl acrylate, 2-acrylamido-2-methylpropane sulfonic acid, and acrylic acid [11,15–19]. In recent years, important researches have been reported on chitosan-clay composites and grafting with monomers for the removal of pollutants [20–30]. So far, no report has been published about chitosan grafting with itaconic acid-methacrylamide (IA-MAm) monomer mixture in the presence of 4,4′-azobis(4-cyanovaleric acid) (ACV), and in the published reports, common radical initiators benzoyl peroxide (BPO) and azobisisobutyronitrile (AIBN) have been used.

In my recent study, chitosan was grafted with a mixture of itaconic acid-methacrylamide-bentonite monomers [31].

In this research, chitosan was grafted with IA-MAm monomer mixture in the presence of ethylene glycol dimethacrylate (EGDMA) and ACV. After characterization by various methods, it was used as an adsorbent of gallic acid (GA) (as a model of a cyclic compound) and Pb^{2+}.

2. Experimental

2.1. Materials

Medium molecular weight CTS (Sigma-Aldrich) and all of chemicals such as IA and MAm as monomers, EGDMA as cross-linker, ACV as radical initiator, GA, Lead acetate and the required solvents were supplied by Merck and were analytical grade and highest purity. Also doubly distilled water has been used in all experiments.

2.2. Instruments

The structure of the composite and the amount of adsorption were investigated by Fourier-transform infrared spectroscopy (FTIR; Bruker Equinox Spectrophotometer with KBr disks), X-ray diffraction (XRD; PW 1730), scanning electron microscopy (SEM; Philips CM120), thermogravimetric analysis (TGA; Church Stretton), atomic absorption spectroscopy (AAS; GBC 932 AA) and UV-Spectrophotometer (Shimadzu 1208).

2.3. Synthesis of composite

0.2 g of chitosan was dissolved in 35 mL of 5 wt.% acetic acid. Then, ACV was dissolved in 5 mL of distilled water and added to the solution. Two monomers of itaconic acid (IA), methacrylamide (MAm) are also added. Finally, ethylene glycol dimethacrylate (EGDMA) is added to the solution as a cross-linker. The contents were placed in a water bath present at 90°C. Finally, the purification was performed with Whatman Filter Paper and washed with fresh methanol and dried at 50°C. By changing the percentage of monomers, initiator concentration, cross-linker concentration and time, optimal conditions were obtained by gravimetrically [32,33].

2.4. Adsorption procedure

Investigation of the adsorption of 50 mg/L of adsorbates with 0.01 g of adsorbent in the total volume of 20 mL, inside Erlenmeyer flask (250 mL) with constant shaker speed (150 rpm) and at a constant temperature of 298 K as a function pH, adsorbate concentration, the amount of adsorbent and time were accomplished. The solutions were then filtered and centrifuged at 3,000 rpm. Residual solution concentration in GA was measured using a UV-Spectrophotometer at λ_{max} = 265 nm using a calibration curve and the residual concentration of Pb^{2+} ions in solution was measured using an AAS instrument at λ_{max} = 217 nm with the help of a calibration curve. Calibration curves for GA and Pb^{2+} were plotted in the concentration range of 5–50 mg/L.

Finally, the adsorbent efficiency was calculated using the calibration curve and the following equation:

$$q = \frac{\left(C_0 - C_e\right)}{m} V \tag{1}$$

where C_0 and C_e are the initial and equilibrium concentrations of adsorbate (mg/L), V total volume of solution (L), m absorbent weight (g) and q is the amount of the adsorbed at the specified time (mg/g) [34].

3. Results and discussion

3.1. Adsorbent synthesis and characterization

According to the preparation method, in a constant amount of monomers (0.1 g) and a change in the weight percentage of two monomers, the best conditions were observed in 0.09 g MAm–0.01 g IA.

The amount of initiator was performed from 0.005 to 0.075 g and the maximum grafting yield was observed in 0.01 g of initiator.

By changing the amount of cross-linker in the range of 1–4 mL, the best grafting yield was obtained in 2 mL. The synthesis time varied from 30 to 120 min and the optimum condition was observed in 45 min. Under optimal conditions of synthesis, the characterization of the composite was studied.

Comparison of chitosan and grafted chitosan FTIR spectra showed the following spectral changes: The main characteristic peaks of pure chitosan are at 3,436 cm^{-1} (O–H stretch), 2,879 cm^{-1} (C–H stretch), 1,605 cm^{-1} (N–H bond), 1,379 cm^{-1} (C–N stretch), 1,089 cm^{-1} (C–O stretch) and 1,155 cm^{-1} (bridge O stretch). In addition to chitosan peaks, 2 new peaks at 3,106 cm^{-1} (N–H stretch of amide) and 1,725 cm^{-1} (C=O stretch of acid) confirm the correlation of 2 monomers IA, MAm to chitosan (Figs. 1 and 2).

TGA results show that after grafting, degradation begins at a lower temperature. As shown in Figs. 3 and 4, chitosan

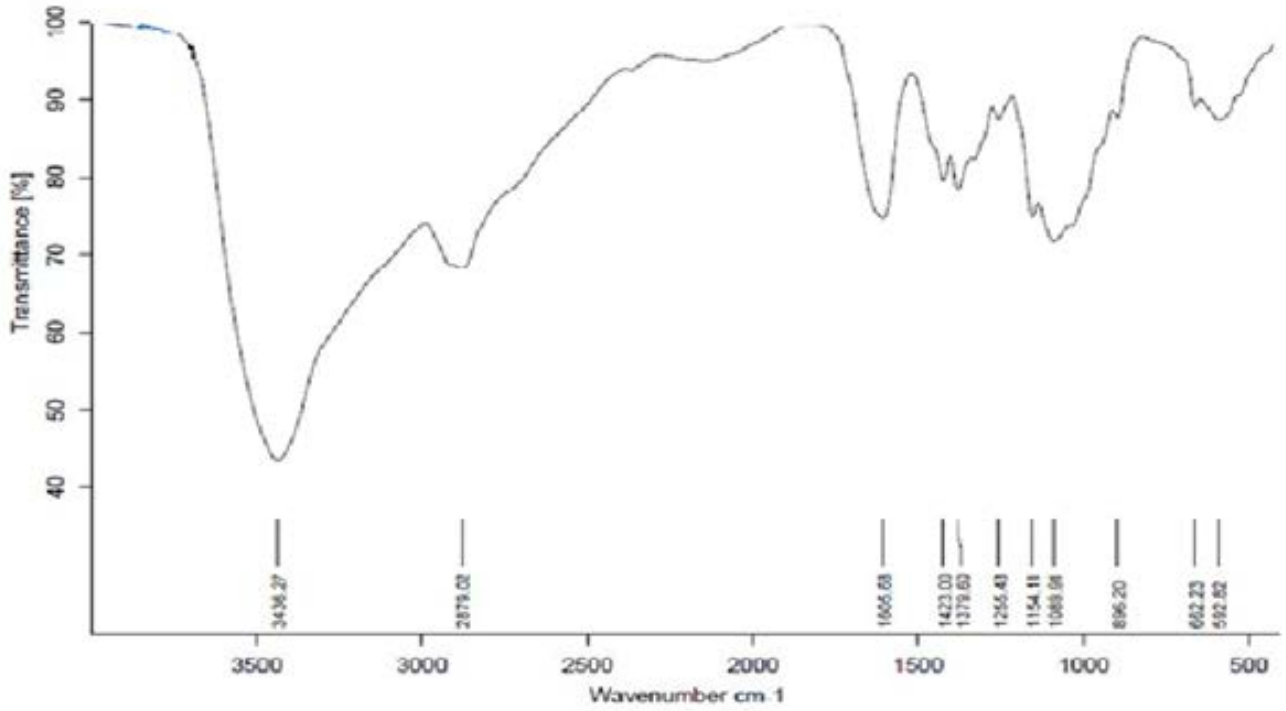

Fig. 1. FTIR spectrum of chitosan.

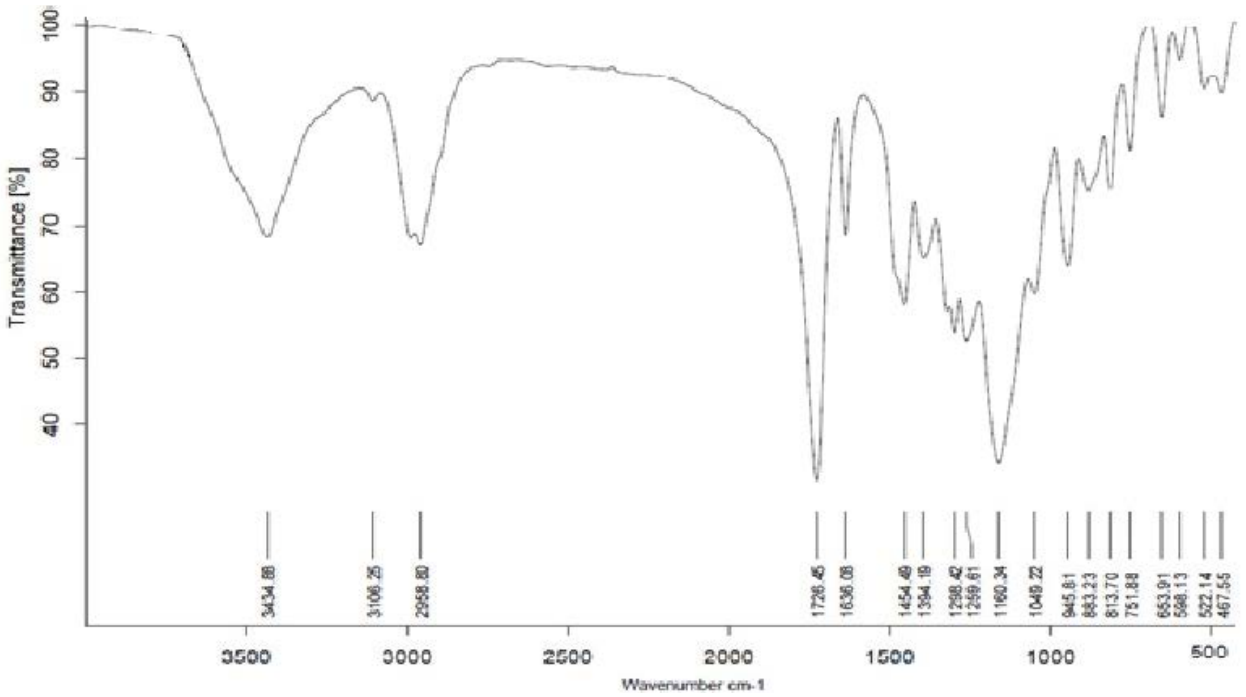

Fig. 2. FTIR spectrum of IA/MAm grafted onto chitosan.

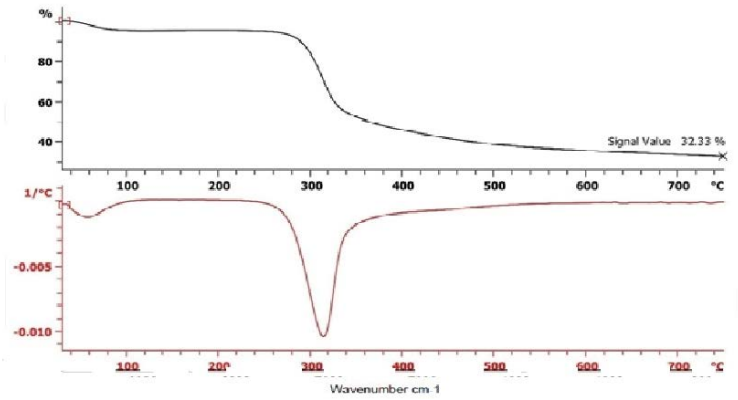

Fig. 3. TGA of chitosan.

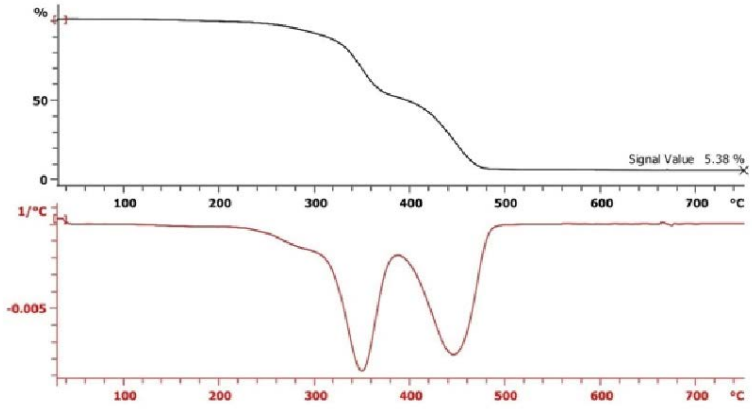

Fig. 4. TGA of IA/MAm mixture grafted onto chitosan.

degradation temperature starts from 300°C and grafted chitosan degradation temperature starts from about 220°C. This is due to the reduction in crystallinity.

The XRD pattern in chitosan shows 2 peaks at 2θ = 10° and 20° indicates high crystallinity. This result is consistent with previous reports [35,36]. The corresponding peaks disappeared after grafting and a weak peak appeared at 2θ = 15° which indicates a decrease in crystallinity and an increase in amorphous structure (Figs. 5 and 6).

SEM image show that the chitosan surface is smooth and dense. But the surface of grafted chitosan with IA and MAm is rough and porous. This image confirms the grafting (Figs. 7 and 8).

3.2. Effect of pH

Under constant conditions of adsorption time (60 min), adsorbent (0.01 g), shaker speed (150 rpm), adsorbate concentration (50 mg/L), total volume (20 mL), temperature 298 K, pH changes from 2.0–10.0, were investigated. The best pH for adsorption of Pb^{2+} ions was recorded at pH = 4.0 and for GA at pH = 3.0. At pH above 6.0, lead precipitates in the form of hydroxide [37].

In the case of GA, due to the presence of functional groups in chitosan and monomers grafted to it, high adsorption was observed in various pH. On the other hand, at alkaline pH, gallic acid is formed as galleate, but at acidic pH, it is possible to bond with the amide group. The best adsorption was recorded at pH = 3.0 (Figs. 9 and 10).

3.3. Effect of time

The effect of contact time on adsorption was studied from 30 to 120 min at the fixation condition of other variables (pH = 4.0 for Pb^{2+} and pH = 3.0 for GA, solution volume = 20 mL, T = 298 K, adsorbent = 0.01 g, adsorbate concentration = 50 mg/L and shaking rate = 150 rpm). As shown in Figs. 11 and 12, the best adsorption time for GA, 60 min and for Pb^{2+}, 75 min were recorded.

3.4. Effect of adsorbate concentration and adsorbent amount

By changing the concentration of adsorbates, from 50 to 400 mg/L, under optimized conditions, experiments were performed. The maximum adsorption at a concentration of 300 mg/L for GA and 150 mg/L for Pb^{2+} were observed. By increasing the amount of adsorbent, the highest adsorption was recorded with 0.02 g for gallic acid and 0.05 g for Pb^{2+}. In the mentioned values, the removal percentage in both cases reached 98%. Figs. 13–16.

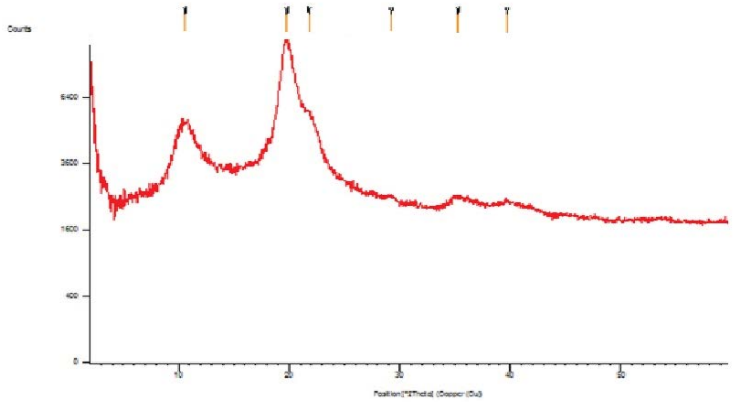

Fig. 5. XRD pattern of chitosan.

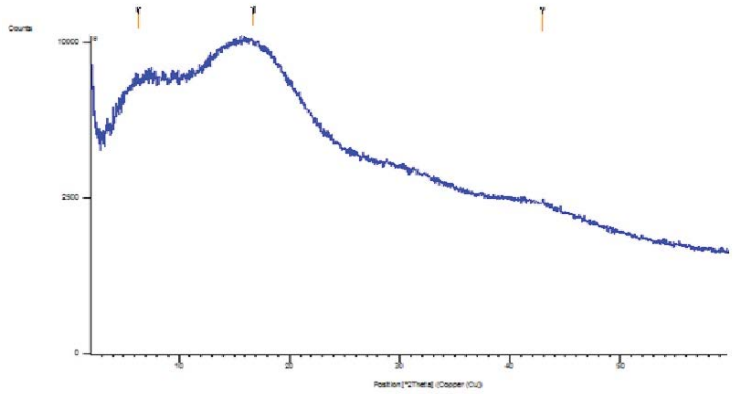

Fig. 6. XRD pattern of IA/MAm mixture grafted onto chitosan.

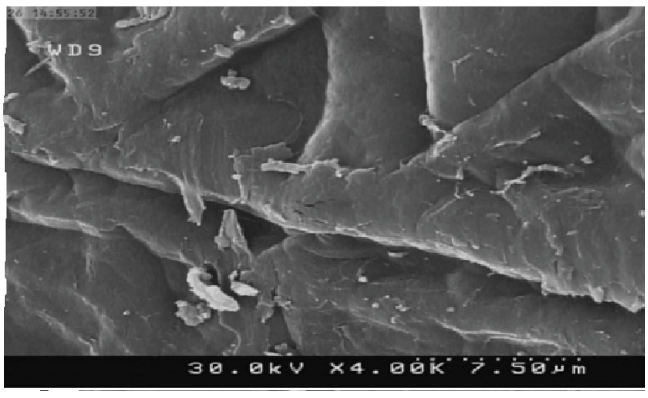

Fig. 7. SEM micrograph of chitosan.

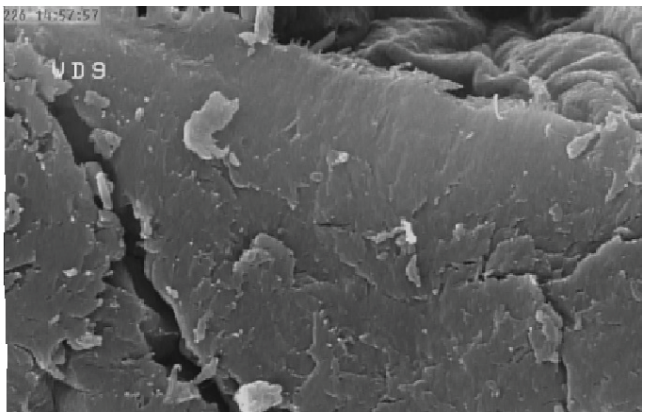

Fig. 8. SEM micrograph of IA/MAm mixture grafted onto chitosan.

The value of q_{max} for GA was 576 and 276 mg/g for Pb^{2+}. Due to the grafting of monomers and the presence of functional groups, the adsorption capacity has increased significantly.

3.5. Adsorption isotherm study

The experimental data were determined according to the commonly used adsorption isotherms, like Langmuir and Freundlich. Langmuir isotherm is based on the hypothesis that point of valence exists on the surface of the adsorbent and that each of these sites is authoritative of one molecule. The Langmuir equation is given as follows [38].

$$\frac{C_e}{q_e} = \frac{1}{q_m b} + \frac{C_e}{q_m} \tag{2}$$

where C_e is the equilibrium concentration (mg/L), q_e is the amount adsorbed at equilibrium (mg/g). q_m and b are

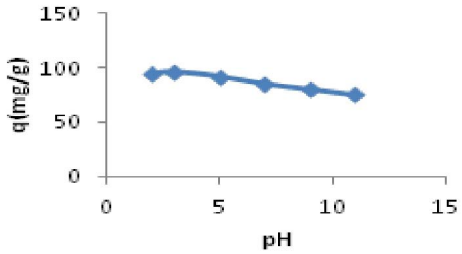

Fig. 9. Effect of pH on the adsorption of GA.

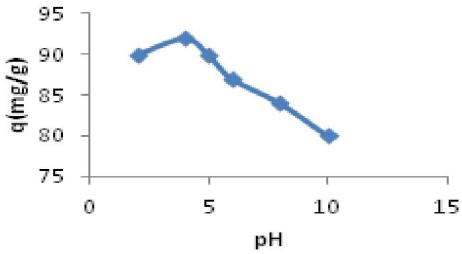

Fig. 10. Effect of pH on the adsorption of Pb^{2+}.

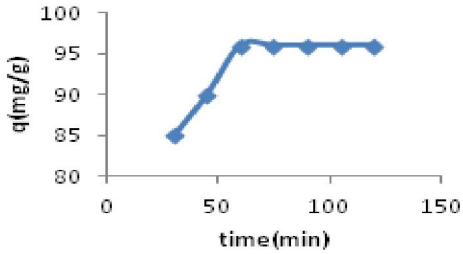

Fig. 11. Effect of contact time on the adsorption of GA.

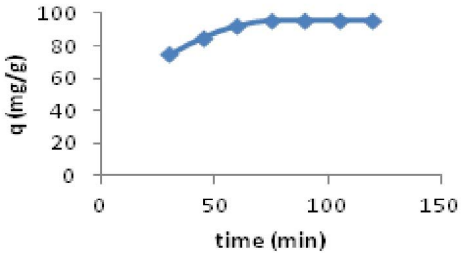

Fig. 12. Effect of contact time on the adsorption of Pb^{2+}.

Langmuir constants depend to adsorption efficiency and energy of adsorption. The linear plots of C_e/q_e vs. C_e identify the applicability of the Langmuir isotherms. The values of q_m and b can be determined from slope and intercepts of the curve.

The Freundlich isotherm is given by the following equation [39].

$$\ln q_e = \ln K_f + \frac{1}{n}\ln C_e \quad (3)$$

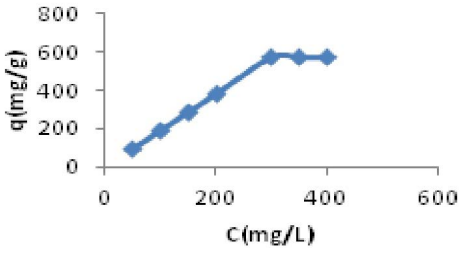

Fig. 13. Effect of GA concentration (mg/L).

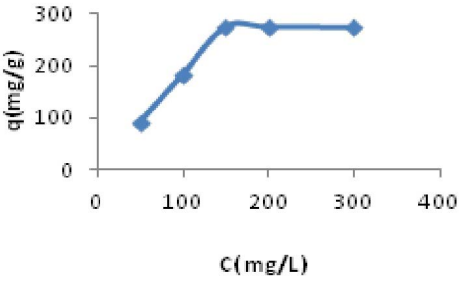

Fig. 14. Effect of Pb^{2+} concentration (mg/L).

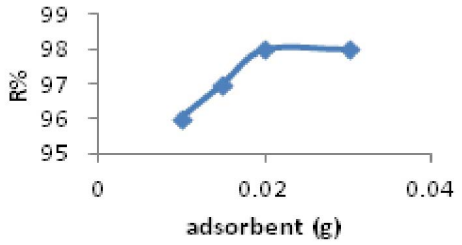

Fig. 15. Effect of adsorbent amount on the adsorption of GA.

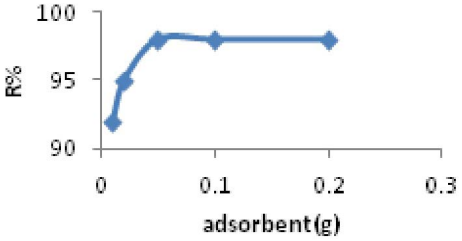

Fig. 16. Effect of adsorbent amount on the adsorption of Pb^{2+}.

where K_f and n are constants the factors affecting the adsorption capacity and strength adsorption, respectively. As can be seen from Figs. 17–20 and Table 2, the best isotherm to justify the adsorption of both adsorbates is the Langmuir isotherm. The correlation coefficient in both cases is higher than R^2 = 0.99. This indicates the homogeneity of the adsorption process on the adsorbent surface [32].

3.6. Adsorption kinetics

Two well-known and important pseudo-first-order, pseudo-second-order kinetic models were used to investigate

Table 1
Percentage of weight loss in the range of 100°C to 700°C

Temperature (°C)	Chitosan	Composite
100	5.11	0.2
200	5.04	1.06
300	17.54	8.67
400	54.58	51.53
500	61.79	94.01
600	64.78	94.38
700	66.77	94.59

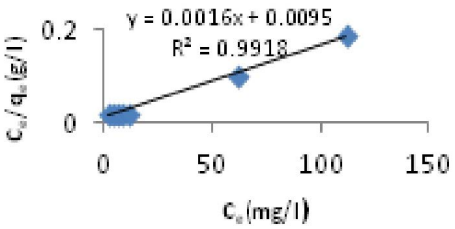

Fig. 17. Langmuir isotherm for GA (T = 298 K).

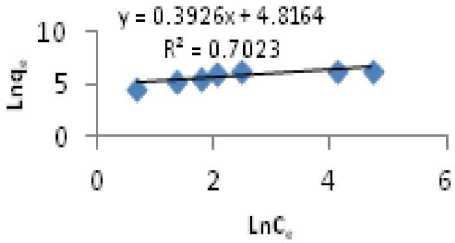

Fig. 18. Freundlich isotherm for GA (T = 298 K).

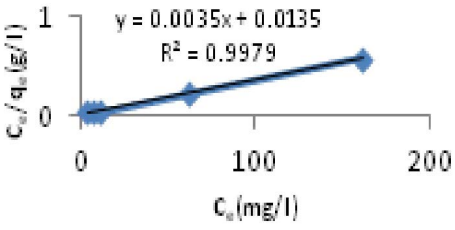

Fig. 19. Langmuir isotherm for Pb^{2+} (T = 298 K).

the adsorption kinetics. Fixed conditions in experiments: 0.01 g of adsorbent, total volume 20 mL, adsorbate concentration 50 mg/L, zero shaker speed, optimal pH 3.0 and 4.0 for lead ions and gallic acid was performed from 5 to 45 min.

Pseudo-first-order: $\ln\left(q_e - q_t\right) = \ln q_e - K_1 t$ (4)

Pseudo-second-order: $\frac{t}{q_t} = \frac{1}{K_2 q_e^2} + \frac{t}{q_e}$ (5)

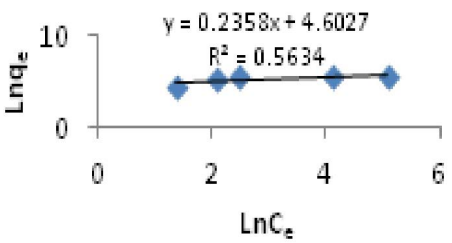

Fig. 20. Freundlich isotherm for Pb^{2+} (T = 298 K).

Table 2
Adsorption isotherm constants

Langmuir constants	K_a (L/mg)	q_m (mg/g)	R^2
Pb^{2+} (298 K)	0.26	285.7	0.9979
Freundlich constants	K_f (mg/g)	n (L/mg)	R^2
Pb^{2+} (298 K)	99.753	4.24	0.5634
Langmuir constants	K_a (L/mg)	q_m (mg/g)	R^2
GA (298 K)	0. 168	625.0	0.9918
Freundlich constants	K_f (mg/g)	n (L/mg)	R^2
GA (298 K)	123.53	2.55	0.7023

where q_e and q_t denote the amounts of metal adsorbed (mg/g) at equilibrium and at time t (min). K_1 (min^{-1}) and K_2 (g/mg·min) are the rate constants of pseudo-first-order and pseudo-second-order models, respectively [40–42].

As shown in Figs. 21–24 and Table 3, in both cases, due to the compatibility of the results with the pseudo-second-order kinetic model, in addition to physical adsorption, chemical adsorption has also been performed [32].

3.7. Thermodynamic parameters

Thermodynamic parameters including Gibbs free energy change ($\Delta G°$), enthalpy change ($\Delta H°$) and entropy change ($\Delta S°$) were evaluated to determine the nature of the adsorption reaction. These parameters were evaluated by the following equations:

$$\Delta G° = \Delta H° - T\Delta S° \quad (6)$$

$$\Delta G° = -RT\ln K_d \quad (7)$$

$$\ln K_d = \frac{\Delta S°}{R} - \frac{\Delta H°}{RT} \quad (8)$$

$$K_d = \frac{q_e}{C_e} \quad (9)$$

where K_d is the equilibrium constant, T is the temperature (K), R is the gas constant. $\Delta H°$ and $\Delta S°$ are the change of enthalpy and entropy and by the help of Van't Hoff plots were determined. Results presented in Figs. 25 and 26 and Tables 4 and 5.

According to the obtained results, the adsorption process is endothermic and spontaneous and due to the positive

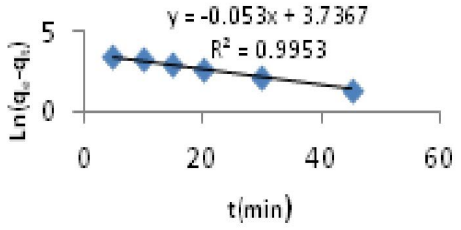

Fig. 21. Pseudo-first-order kinetics for GA.

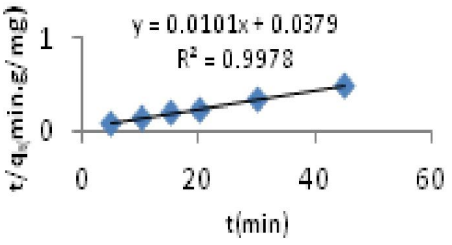

Fig. 22. Pseudo-second-order kinetics for GA.

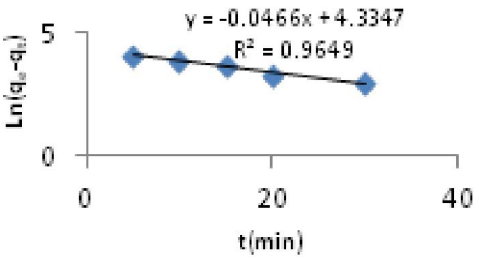

Fig. 23. Pseudo-first-order kinetics for Pb^{2+}.

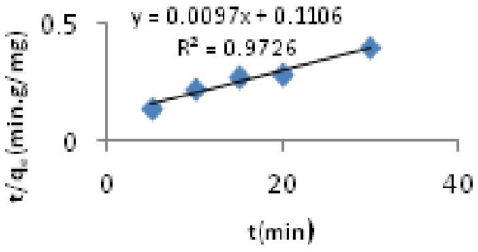

Fig. 24. Pseudo-second-order kinetics for Pb^{2+}.

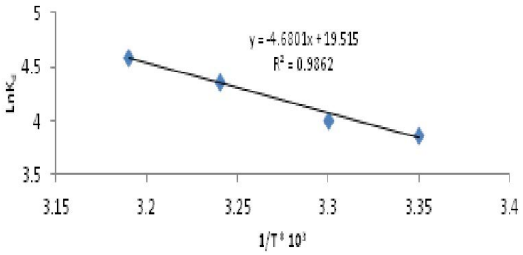

Fig. 25. Van't Hoff plot for thermodynamic parameters of GA.

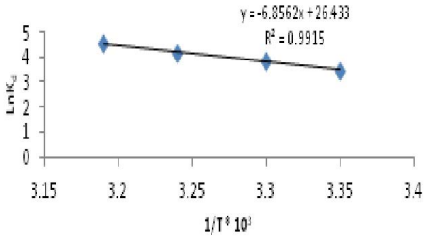

Fig. 26. Van't Hoff plot for thermodynamic parameters of Pb^{2+}.

Table 4
Thermodynamic parameters at different temperatures for Pb^{2+}

T (K)	$\Delta H°$ (kJ/mol)	$\Delta S°$ (kJ/mol·K)	$\Delta G°$ (kJ/mol)
298	18.542	71.487	–5.750
303			–6.896
308			–7.800
313			–8.995

Table 5
Thermodynamic parameters at different temperatures for GA

T (K)	$\Delta H°$ (kJ/mol)	$\Delta S°$ (kJ/mol·K)	$\Delta G°$ (kJ/mol)
298	6.619	27.603	–5.202
303			–5.652
308			–6.633
313			–7.371

Table 3
Adsorption kinetic parameters

Pseudo-first-order kinetic model (Pb^{2+})			Pseudo-second-order kinetic model (Pb^{2+})		
q_e (mg/g)	K_1 (min^{-1})	R^2	q_e (mg/g)	K_2 (g/mg·min)	R^2
76.30	0.046	0.9649	103.09	0.00085	0.9726
Pseudo-first-order kinetic model (GA)			Pseudo-second-order kinetic model (GA)		
q_e (mg/g)	K_1 (min^{-1})	R^2	q_e (mg/g)	K_2 (g/mg·min)	R^2
41.96	0.053	0.9953	100	0.0026	0.9978

Table 6
Application of carbonized datestone for the removal of Pb^{2+} in groundwater samples

Water samples	Before adsorption	After adsorption	% removal of Pb^{2+}	RSD (%)
	Pb^{2+} in mg/L	Pb^{2+} in mg/L		
Tap water	7.33	1.61	78.03	2.2
Groundwater	9.33	2.11	77.37	2.3
Industrial water from Charmshar	20.78	4.80	76.90	2.4
Quds Industrial Town	21.25	4.95	76.70	2.4

Table 7
Comparison of this study with some of the methods reported in the literature

Adsorbent	Adsorbate	Adsorption capacity (mg/g)	References
PEO/chitosan	Pb^{2+}	237.2	[45]
Chitosan/HAp	Pb^{2+}	296.7	[46]
Fe_2O_3/Al_2O_3	Pb^{2+}	23.75	[47]
PEI/PES	Pb^{2+}	94.34	[48]
Chitosan/GO	Pb^{2+}	461.3	[49]
Chitosan-vanilin	Pb^{2+}	66.23	[50]
Hydrothermal biochar	Pb^{2+}	133.2	[51]
Lactic acid bacteria	Pb^{2+}	10.51	[52]
Magnetic adsorbent	Pb^{2+}	70.4	[53]
Citrus grandis	Pb^{2+}	207.2	[54]
Magnetic chitosan	Pb^{2+}	175.4	[55]
PET fibers	GA	38.2	[56]
Magnetic resin	GA	30.75	[57]
This study	Pb^{2+}, GA	276,576	

entropy, confirms the appropriate interaction of adsorbent and adsorbate.

3.8. Desorption and regeneration study

Desorption was performed by 0.1 M HNO_3. Adsorption and desorption were performed 5 times and the adsorbent efficiency reached approximately 90% [33,43,44].

3.9. Proposed adsorbent application in wastewater samples

At the best condition of adsorbent (time = 75 min, pH = 4.0, adsorbent = 0.05 g), the adsorbent efficiency in the removal of the Pb^{2+} was investigated. Percentage of removal of Pb^{2+} ions in samples of well water, Charmshahr industrial water and other water samples were about 77% (Table 6). The presence of other ions in real water samples slightly interfered with the adsorption of Pb^{2+} ions under optimal conditions. Hence, the percentage of Pb^{2+} ion removal in groundwater samples was less than the value obtained using Box–Behnken statistical analysis.

3.10. Comparison of this method with previous methods

Comparison of this method with other methods shows that the adsorption speed and capacity are high and the adsorption time is shorter. Therefore, it is an advantage over the previous methods. Some results can be seen in Table 7.

4. Conclusion

In this study, a new adsorbent based on chitosan grafted with a mixture of IA-MAm monomers was prepared and characterized. Its efficiency in Pb^{2+} and GA adsorption was evaluated according to the batch technique. Effective parameters on adsorption were optimized. In acidic pH, high adsorption efficiency was observed. Consistency with the Langmuir isotherm model and the pseudo-second-order kinetic model showed that the adsorption process of both adsorbates is homogeneous, monolayer and chemical. On the other hand, the results of adsorption–desorption tests showed that the adsorbent has good efficiency and reproducibility. The adsorbent efficiency in the removal of lead ions in industrial effluents was appropriate and acceptable.

Conflict of interest

The authors declare that they have no conflict of interest. The datasets generated during and/or analysed during the current study are available from the corresponding author on reasonable request.

References

[1] L.L. Hench, Biomaterials: a forecast for the future, Biomaterials, 19 (1998) 1419–1423.
[2] F.-C. Wu, R.-L. Tseng, R.-S. Juang, A review and experimental verification of using chitosan and its derivatives as adsorbents for selected heavy metals, J. Environ. Manage., 91 (2010) 798–806.
[3] M. Jaishankar, T. Tseten, N. Anbalagan, B.B. Mathew, K.N. Beeregowda, Toxicity, mechanism and health effects of some heavy metals, Interdiscip. Toxicol., 7 (2014) 60–72.
[4] M. Iqbal, *Vicia faba* bioassay for environmental toxicity monitoring: a review, Chemosphere, 144 (2016) 785–802.
[5] K.G. Bhattacharyya, S.S. Gupta, Adsorption of a few heavy metals on natural and modified kaolinite and montmorillonite: a review, Adv. Colloid Interface Sci., 140 (2008) 114–131.
[6] F. Fenglian, Q. Wang, Removal of heavy metal ions from wastewaters: a review, J. Environ. Manage., 92 (2011) 407–418.
[7] S.S. Pillai, B. Deepa, E. Abraham, N. Girija, P. Geetha, L. Jacob, M. Koshy, Biosorption of Cd(II) from aqueous solution using xanthated nano banana cellulose: equilibrium and kinetic studies, Ecotoxicol. Environ. Saf., 98 (2013) 352–360.

[8] W. Cui, P. Fang, K. Zhu, Y. Mao, C. Gao, Y. Xie, J. Wang, W. Shen, Hydrogen-rich water confers plant tolerance to mercury toxicity in alfalfa seedlings, Ecotoxicol. Environ. Saf., 105 (2014) 103–111.
[9] H.S. Blair, J. Guthrie, T.-K. Law, P. Turkington, Chitosan and modified chitosan membranes I. Preparation and characterisation, J. Appl. Polym. Sci., 33 (1987) 641–656.
[10] A. Lagos, J. Reyes, Grafting onto chitosan. I. Graft copolymerization of methyl methacrylate onto chitosan with Fenton's reagent (Fe^{2+}–H_2O_2) as a redox initiator, J. Polym. Sci., Part A: Polym. Chem., 26 (1988) 985–991.
[11] M. Yazdani-Pedram, J. Retuert, Homogeneous grafting reaction of vinyl pyrrolidone onto chitosan, J. Appl. Polym. Sci., 63 (1997) 1321–1326.
[12] K. Kurita, A. Yoshida, Y. Koyama, Studies on chitin. 13. New polysaccharide/polypeptide hybrid materials based on chitin and poly(.gamma.-methyl L-glutamate), Macromolecules, 21 (1988) 1579–1583.
[13] Y. Shigeno, K. Kondo, K. Takemoto, Functional monomers and polymers. 90 radiation-induced graft polymerization of styrene onto chitin and chitosan, J. Macromol. Sci. Part A. Chem., 17 (1982) 571–583.
[14] L. Pengfei, Z. Maolin, W. Jilan, Study on radiation-induced grafting of styrene onto chitin and chitosan, Radiat. Phys. Chem., 6 (2001) 149–153.
[15] D.K. Singh, A.R. Ray, Radiation-induced grafting of N,N′-dimethylaminoethylmethacrylate onto chitosan films, J. Appl. Polym. Sci., 66 (1997) 869–877.
[16] D.K. Singh, A.R. Ray, Characterization of grafted chitosan films, Carbohydr. Polym., 36 (1998) 251–255.
[17] D.K. Singh, A.R. Ray, Controlled release of glucose through modified chitosan membranes, J. Membr. Sci., 155 (1999) 107–112.
[18] A.M.K. Najjar, W.M.Z.W. Yunus, M.B. Ahmad, M.Z. Ab. Rahman, Preparation and characterization of poly(2-acrylamido-2-methylpropane-sulfonic acid) grafted chitosan using potassium persulfate as redox initiator, J. Appl. Polym. Sci., 77 (2000) 2314–2318.
[19] M. Yazdani-Pedram, J. Retuert, R. Quijada, Hydrogels based on modified chitosan, 1. Synthesis and swelling behavior of poly(acrylic acid) grafted chitosan, Macromol. Chem. Phys., 201 (2000) 923–930.
[20] G.Z. Kyzas, P.I. Siafaka, D.A. Lambropoulou, N.K. Lazaridis, D.N. Bikiaris, Poly(itaconic acid)-grafted chitosan adsorbents with different cross-linking for Pb(II) and Cd(II) uptake, Langmuir, 30 (2014) 120–131.
[21] J.A. Sirviö, A.M. Kantola, S. Komulainen, S. Filonenko, Aqueous modification of chitosan with itaconic acid to produce strong oxygen barrier film, Biomacromolecules, 22 (2021) 2119–2128.
[22] N.B. Milosavljević, N.Z. Milašinović, I.G. Popović, J.M. Filipović, M.T. Kalagasidis Krušić, Preparation and characterization of pH-sensitive hydrogels based on chitosan, itaconic acid and methacrylic acid, Polym. Int., 60 (2011) 443–452.
[23] N.B. Milosavljević, M.Đ. Ristić, A.A. Perić-Grujić, J.M. Filipović, S.B. Štrbac, Z.Lj. Rakočević, M.T. Kalagasidis Krušić, Sorption of zinc by novel pH-sensitive hydrogels based on chitosan, itaconic acid and methacrylic acid, J. Hazard. Mater., 192 (2011) 846–854.
[24] F. Shakib, A.D. Koohi, A.K. Pirzaman, Adsorption of methylene blue by using novel chitosan-g-itaconic acid/bentonite nanocomposite - equilibrium and kinetic study, Water Sci. Technol., 75 (2017) 1932–1943.
[25] S. Dan, S. Banivaheb, H. Hashemipour, M. Kalantari, Synthesis, characterization and absorption study of chitosan-g-poly(acrylamide-co-itaconic acid) hydrogel, Polym. Bull., 78 (2021) 1887–1907.
[26] A.M. Awwad, M.A. Amer, Adsorption of Pb(II), Cd(II), and Cu(II) ions onto SiO_2/kaolinite/Fe_2O_3 composites: modeling and thermodynamics properties, Chem. Int., 8 (2022) 95–100.
[27] A.M. Awwad, M.W. Shammout, M.W. Amer, $Fe(OH)_3$/kaolinite nanoplatelets: equilibrium and thermodynamic studies for the adsorption of Pb(II) ions from aqueous solution, Chem. Int., 7 (2021) 90–102.
[28] A.M. Awwad, N.M. Salem, M.W. Amer, M.W. Shammout, Adsorptive removal of Pb(II) and Cd(II) ions from aqueous solution onto modified Hiswa iron-kaolin clay: equilibrium and thermodynamic aspects, Chem. Int., 7 (2021) 139–144.
[29] A.M. Awwad, M.W. Amer, M.M. Al-Aqarbeh, TiO_2-kaolinite nanocomposite prepared from the Jordanian Kaolin clay: adsorption and thermodynamics of Pb(II) and Cd(II) ions in aqueous solution, Chem. Int., 6 (2020) 168–178.
[30] A. Kausar, K. Naeem, T. Hussain, Zill-i-Huma Nazli, H.N. Bhatti, F. Jubeen, A. Nazir, M. Iqbal, Preparation and characterization of chitosan/clay composite for direct Rose FRN dye removal from aqueous media: comparison of linear and non-linear regression methods, J. Mater. Res. Technol., 8 (2019) 1161–1174.
[31] F. Azizinezhad, Surface adsorption of Pb^{2+} ions from aqueous solutions using chitosan grafted with a mixture of IA-MAm/bentonite, Int. J. Environ. Anal. Chem., (2022), doi: 10.1080/03067319.2021.2023514.
[32] T.S. Anirudhan, S. Rijithy, A.R. Tharun, Adsorptive removal of thorium(IV) from aqueous solutions using poly(methacrylic acid)-grafted chitosan/bentonite composite matrix: process design and equilibrium studies, Colloids Surf., A, 368 (2010) 13–22.
[33] M. Sadeghi, Synthesis and swelling behaviors of graft copolymer based on chitosan-g-poly(AA-co-HEMA), Int. J. Chem. Eng. Appl., 1 (2010) 354–358.
[34] F. Azizinezhad, Surface adsorption of an acidic dye (erionyl blue) on poly(ethylene terephthalate)-grafted-methyl methacrylate/acrylic acid, Eur. J. Exp. Biol., 4 (2014) 543–549.
[35] S. Tripathi, G.K. Mehrotra, P.K. Dutta, Physicochemical and bioactivity of cross-linked chitosan–PVA film for food packaging applications, Int. J. Biol. Macromol., 45 (2009) 372–376.
[36] K. Saita, S. Nagoka, T. Shirosaki, M. Horikawa, S. Matsuda, H. Ihara, Preparation and characterization of dispersible chitosan particles with borate crosslinking and their antimicrobial and antifungal activity, Carbohydr. Res., 349 (2012) 52–58.
[37] Y. Tan, M. Chen, Y. Hao, High efficient removal of Pb(II) by amino-functionalized Fe_3O_4 magnetic nano-particles, Chem. Eng. J., 191 (2012) 104–111.
[38] A. Balouch, M. Kolachi, F.N. Talpur, H. Khan, M.I. Bhanger, Sorption kinetics, isotherm and thermodynamic modeling of defluoridation of groundwater using natural adsorbents, Am. J. Anal. Chem., 4 (2013) 221–228.
[39] H. Freundlich, Über die adsorption in lösungen, Zeitschrift, Physikalische Chemie, 57 (1906) 385–470.
[40] S. Lagergren, Zur theorie der sogenannten adsorption gel.oster stoffe, Kungliga Svenska Vetenskapsakademiens, Handlingar, 24 (1898) 1–39.
[41] Y.S. Ho, G. McKay, Pseudo-second-order model for sorption processes, Process Biochem., 34 (1999) 451–465.
[42] Y.S. Ho, Adsorption of Heavy Metals from Waste Streams by Peat, Ph.D. Thesis, University of Birmingham, Birmingham, UK, 1995.
[43] M. Chaari, M. Feki, M. Medhioub, J. Bouzid, E. Fakhfakh, F. Jamoussi, Adsorption of a textile dye "Indanthrene Blue RS (C.I. Vat Blue 4)" from aqueous solutions onto smectite-rich clayey rock, J. Hazard. Mater., 172 (2009) 1623–1628.
[44] A. Borzou, M. Kalbasi, M. Hoodaji, M. Abdouss, A. Mohammadi, Adsorption–desorption behavior of cadmium and lead by modified poly ethylene terephthalate fiber, Bull. Environ. Pharmacol. Life Sci., 3 (2014) 209–216.
[45] M. Aliabadi, M. Irani, J. Ismaeili, H. Piri, M.J. Parnian, Electrospun nanofiber membrane of PEO/chitosan for the adsorption of nickel, cadmium, lead and copper ions from aqueous solution, Chem. Eng. J., 220 (2013) 237–243.
[46] M. Aliabadi, M. Irani, J. Ismaeili, S. Najafzadeh, Design and evaluation of chitosan/hydroxyapatite composite nanofiber membrane for the removal of heavy metal ions from aqueous solution, J. Taiwan Inst. Chem. Eng., 45 (2014) 518–526.
[47] A. Mahapatra, B.G. Mishra, G. Hota, Electrospun Fe_2O_3-Al_2O_3 nanocomposite fibers as efficient adsorbent for removal of heavy metal ions from aqueous solution, J. Hazard. Mater., 258 (2013) 116–123.

[48] M. Min, L. Shen, G. Hong, M. Zhu, Y. Zhang, X. Wang, Y. Chen, B.S. Hsiao, Micro-nano structure poly(ether sulfones)/poly(ethyleneimine) nanofibrous affinity membranes for adsorption of anionic dyes and heavy metal ions in aqueous solution, Chem. Eng. J., 197 (2012) 88–100.
[49] H.H. Najafabadi, M. Irani, L. Roshanfekr Rad, A. Heydari Haratameh, I. Haririan, Removal of Cu^{2+}, Pb^{2+} and Cr^{6+} from aqueous solutions using a chitosan/graphene oxide composite nanofibrous adsorbent, RSC Adv., 5 (2015) 16532–16539.
[50] F. Alakhras, H. Al-Shahrani, E. Al-Abbad, F. Al-Rimawi, N. Ouerfelli, Removal of Pb(II) metal ions from aqueous solutions using chitosan-vanillin derivatives of chelating polymers, Pol. J. Environ. Stud., 28 (2019) 1523–1534.
[51] B. Wang, J. Yu, H. Liao, W. Zhu, P. Ding, J. Zhao, Adsorption of lead(II) from aqueous solution with high efficiency by hydrothermal biochar derived from honey, Int. J. Environ. Res. Public Health, 17 (2020) 3441, doi: 10.3390/ijerph17103441.
[52] S. Wierzba, Removal of Cu(II) and Pb(II) from aqueous solutions by lactic acid bacteria, Proc. ECOpole, 9 (2015) 505–512.
[53] Y. Xu, I.-K. Yoo, Removal of lead from water solution by reusable magnetic adsorbent incorporating selective lead-binding peptide, Appl. Biosci. Bioeng., *10* (2020) 6418–6428.
[54] L.B.L. Lima, N. Priyantha, Y.C. Lu, N.A.H.M. Zaidia, Adsorption of heavy metal lead using *Citrus grandis* (Pomelo) leaves as low-cost adsorbent, Desal. Water Treat., 166 (2019) 44–52.
[55] N. Salehi, A. Moghimi, H.R. Shahbazi, Preparation of cross-linked magnetic chitosan with methionine-glutaraldehyde for removal of heavy metals from aqueous solutions, Int. J. Environ. Anal. Chem., 102 (2022) 2305–2321.
[56] E. Fathi, F. Azizinezhad, M. Shabani, Surface adsorption of gallic acid by poly(ethylene terephthalate) fibers grafted 2-hydroxy propyl methacrylate/acrylamide, J. Appl. Chem., 12 (2016) 147–160.
[57] L. Ding, C. Guo, Y. Zhu, J. Ma, Y. Kong, M. Zhong, Q. Cao, H. Zhang, Adsorptive removal of gallic acid from aqueous solution onto magnetic ion exchange resin, Water Sci. Technol., 81 (2020) 1479–1493.